Adversarial Cooperative Rationalization: The Risk of Spurious Correlations in Even Clean Datasets

Wei Liu [1] **Zhongyu Niu** [1] **Lang Gao** [1] **Zhiying Deng** [2] **Jun Wang** [3] **Haozhao Wang** [1] **Ruixuan Li** [1]

Abstract

This study investigates the self-rationalization framework constructed with a cooperative game, where a generator initially extracts the most informative segment from raw input, and a subsequent predictor utilizes the selected subset for its input. The generator and predictor are trained collaboratively to maximize prediction accuracy. In this paper, we first uncover a potential caveat: such a cooperative game could unintentionally introduce a sampling bias during rationale extraction. Specifically, the generator might inadvertently create an incorrect correlation between the selected rationale candidate and the label, even when they are semantically unrelated in the original dataset. Subsequently, we elucidate the origins of this bias using both detailed theoretical analysis and empirical evidence. Our findings suggest a direction for inspecting these correlations through attacks, based on which we further introduce an instruction to prevent the predictor from learning the correlations. Through experiments on six text classification datasets and two graph classification datasets using three network architectures (GRUs, BERT, and GCN), we show that our method not only significantly outperforms recent rationalization methods, but also achieves comparable or even better results than a representative LLM (llama3.1-8b-instruct). Code: https://github.com/jugechengzi/Rationalization-A2I.

[1]School of Computer Science and Technology, Huazhong University of Science and Technology [2]Faculty of Artificial Intelligence in Education, Central China Normal University [3]iWudao Tech. Correspondence to: Zhiying Deng <zhiyingdzy@gmail.com>, Jun Wang <jwang@iwudao.tech>, Haozhao Wang <hz_wang@hust.edu.cn>, Ruixuan Li <rxli@hust.edu.cn>.

Proceedings of the 42nd International Conference on Machine Learning, Vancouver, Canada. PMLR 267, 2025. Copyright 2025 by the author(s).

1. Introduction

With the success of deep learning, there are growing concerns over the model interpretability. In contrast to post-hoc methods, self-explaining techniques typically offer increased transparency (Lipton, 2018) and faithfulness (Yu et al., 2021), as the prediction is made based on the explanation itself. There is a stream of research that has exposed the unreliability of post-hoc explanations and called for self-explanatory methods (Rudin, 2019; Ghassemi et al., 2021; Ren et al., 2024).

In this study,our primary focus is on investigating a general model-agnostic self-explaining framework called Rationalizing Neural Predictions (RNP, also known as rationalization) (Lei et al., 2016), which with its variants has become one of the mainstream methods to facilitate the interpretability of NLP models (Sha et al., 2021; Yu et al., 2021; Liu et al., 2023a;b; 2024a;b), and also holds the potential to be applied to image classification (Yuan et al., 2022) and graph neural networks (Luo et al., 2020). RNP utilizes a cooperative game involving a generator and a predictor. This game is designed with a focus on "data-centric" (i.e., it is to explain the connection between a text and the (model-agnostic) task label, rather than explaining the output of a specific model) feature importance. The generator first identifies the most informative part of the input, termed the rationale. Subsequently, the rationale is transmitted to the predictor to make predictions, as illustrated in Figure 1. The generator and predictor are trained cooperatively to maximize prediction accuracy. Apart from its use for interpretability, some recent studies find that rationalization can also serve as a method for data cleaning. The extracted (Z, Y) pairs can act as a new dataset, and trained with such a cleaned dataset, a predictor may be more robust (Chen et al., 2022) and generalizable (Wu et al., 2022; Gui et al., 2023), thanks to the removal of task-irrelevant, harmful information.

Our research starts with a special empirical observation. We first observe that, even if we remove "maximizing the prediction accuracy" from the generator's objective (thus it selects some random noise), the predictor can still be trained to get very high accuracy with these randomly selected spurious rationales (the orange line in Figure 3(a) of §4.1). This phenomenon then leads to a trust concern: whether

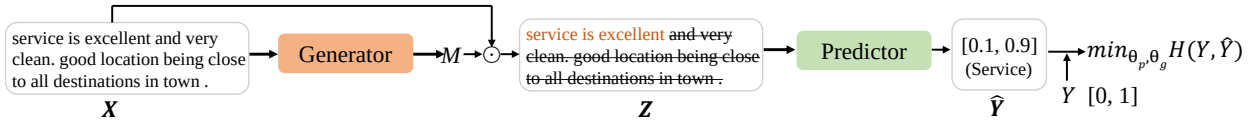

Figure 1. The standard rationalization framework RNP. The task in this figure is binary sentiment classification about hotels' service. $X, Z, \hat{Y}, Y$ represent the input, the selected rationale candidate, the prediction, and the classification label. M is a sequence of binary masks. θ_g, θ_p are the parameters of the generator and the predictor.

Task: Binary sentiment classification
Label (about the beer's appearance): Positive. **Prediction**: Positive.
Input: a - murky , semi-opaque honey . low head . s -earthy. plantains , pineapple rind , apricot t - earthy hay and pepper . touch or orange . cilantro . honey . very saison-like . m - medium body . nice carbonation . balanced semi-dry finish . o - nice flavor profile .
Rationale selected by RNP: [“.”]

Figure 2. A cherry-picked example of the generator-added spurious correlation. The underlined text is human-annotated rationale. The text in red is the rationale selected by RNP. *Example 1*: from a positive input X^1 with a label 1, the generator selects a rationale Z^1 that includes the pattern “.”; and for a negative input X^0 with a label 0, the generator selects a rationale Z^0 that does not include“.”. And subsequently, the predictor considers the presence or absence of “.” as an indicative feature for positive classification.

the extracted rationale is really responsible for the label in the original dataset (i.e., although the extracted rationale is considered faithful to the model's prediction by previous research, is it faithful to the model-agnostic dataset?). This problem is important because explanations should also be aligned with their social attribution (Jacovi & Goldberg, 2020; 2021).

We then shed light on the source of this problem. Typically, we call a pattern T is **t**rivial if it is independent with Y in the original dataset: $P(Y|T) = P(Y)$. However, due to the potential bias of the generator's sampling, T can be correlated with Y in the sampled (Z, Y) pairs. Figure 2 provides a (cherry-picked) practical example of it.

We further explore the origins of this issue and discover that it stems from an approximation that was overlooked in previous research: taking a series of (Y, Z) pairs sampled by the generator as an approximation of $P(Y, Z)$ (while it should actually be $P(Y, Z|g)$, and note that $Y \perp\!\!\!\perp Z \not\Rightarrow Y \perp\!\!\!\perp Z|g$). In fact, this problem can be seen as a type of spurious correlation. But notably, the perspective of this paper is totally different from the traditional causality research for spurious correlations. Existing research on causality has primarily focused on spurious correlations inherent in the dataset. However, our research investigates a further question: *if the dataset itself is clean and lacks spurious correlations, could the selection process of the generator introduce additional spurious correlations?*

This study tries to address this kind of correlations with two steps: inspection and instruction. We first theoretically show that if a predictor classifies based on a trivial pattern T that is associated with the category label Y due to the sampling of the generator, we can always find an attacker to inspect the trivial pattern. Then, to prevent the predictor from learning such a correlation (which would make the generator further enhance it), we manually adjust the distribution of the trivial pattern from $P(Y|T, g)$ to $P(Y)$ (in fact, it should be $P(Y|T)$, but we have $P(Y|T) = P(Y)$ for the attacker identified trivial pattern T) to provide instructions that enable the predictor to learn the correct information, thereby giving the generator the correct feedback. Formal introduction of our method will appear in §4.2. We provide a toy example in Appendix A.2 to give readers a quick intuitive understanding of our method.

Our contributions include: (a) We identify a new type of spurious correlation, and we systematically analyze how it can arise in even clean datasets with both theoretical support and empirical verification. (b) A practical solution. We design an attacker to both inspect whether the predictor has learnt from the spurious correlation and instruct the predictor not to learn from it. (c) We design various experiments to verify the existence of the generator added spurious correlation, the effectiveness of the inspection, and the effectiveness of the instruction.

2. Related work

Rationalization. The basic cooperative framework of rationalization named RNP (Lei et al., 2016) is flexible and offers a unique advantage: certification of exclusion, which means any unselected input is guaranteed to have no contribution to prediction, making it important to the NLP community (Yu et al., 2021). Based on it, many methods have been proposed to improve RNP from different aspects. Bao et al. (2018) used Gumbel-softmax to do the reparameterization for binarized selection. Bastings et al. (2019) replaced the Bernoulli sampling distributions with rectified Kumaraswamy distributions. Jain et al. (2020) disconnected the training regimes of the generator and predictor networks using a saliency threshold. Paranjape et al. (2020) imposed a discrete bottleneck objective to balance the task performance and the rationale length. Liu et al. (2025) replaced the cross-entropy loss with

the final-layer representation norm. DeYoung et al. (2020) proposed a benchmark that can be used for supervised rationale extraction. Inter_RAT (Yue et al., 2023) tried to use backdoor adjustment to alleviate the spurious correlations in the raw dataset. DR (Liu et al., 2023c) assigned different learning rates to the generator and the predictor. Hase et al. (2020) explored better metrics for evaluation. Rajagopal et al. (2021) used phrase-based concepts to conduct a self-explaining model. Other methods like data augmentation with pretrained models (Plyler et al., 2021), training with human-annotated rationales (Chan et al., 2022), injecting noise to the selected rationales (Storek et al., 2023), have also been tried.

Prior to our work, a series of studies had observed a phenomenon termed degeneration, whose origin can also be attributed to the spurious correlation we investigate in this study. Degeneration means that, the predictor is too powerful to recognize any trivial patterns that are distinguishable in rationales with opposite labels. As a result, the generator may collude with the predictor to select the trivial patterns rather than the true semantics as the rationales (Yu et al., 2019). Previous methods seek to regularize the model using supplementary modules which have access to the information of the full text (Yu et al., 2019; Huang et al., 2021; Yu et al., 2021; Liu et al., 2022) such that the generator and the predictor will not overfit uninformative rationales. Among them, FR achieves the strongest improvements on addressing degeneration by sharing a unified encoder between the generator and predictor to regularize each other. And it will be included in our baselines. However, although these methods have been proposed to fix the observed problem, the origin of this problem is not well explored. Sometimes they can still fail. For example, Zheng et al. (2022) argued with both philosophical perspectives and empirical evidence that the degeneration problem is much more complex than we used to think and some of the above methods cannot promise no-degeneration. In fact, this phenomenon is similar to what we discuss and can also be seen as one of the problems stems from taking $P(Y,Z|g)$ as $P(Y,Z)$, highlighting the importance of rectifying the bias in approximating $P(Y,Z|g)$ as $P(Y,Z)$.

We also briefly discuss the potential impact of rationalization in the era of LLMs in Appendix A.1. We compare our method against a representative LLM (llama-3.1-8b-instruct) in Appendix D.

3. Background of the rationalization task

Unless otherwise specified, uppercase letters represent random variables, while lowercase letters correspond to their values. For simplicity, we do not distinguish between vectors and scalars. We consider the classification task. We have a classification dataset $\mathcal{D}$, which can be seen as a collection of samples drawn from the true data distribution $P(X,Y)$. $X = X_{1:l}$ is the input text sequence of length l, and Y represent the classes in the dataset (note that a discrete label can also seen as representing a distribution like [0,1]). By enumerating X, we can get $P(Y|X)$, which is the distribution that a normal non-interpretable classifier working on $\mathcal{D}$ needs to approximate. Rationalization consists of a generator $f_g(\cdot)$ (or g for conciseness) and a predictor $f_p(\cdot)$, with θ_g, θ_p being their parameters.

For $(X,Y) \sim \mathcal{D}$, the generator first outputs a sequence of binary mask $M = f_g(X) = M_{1:l} \in \{0,1\}^l$ (in practice, the generator first outputs a Bernoulli distribution for each token and the mask for each token is independently sampled using gumbel-softmax). Then, it forms the rationale candidate Z by the element-wise product:

$$Z = M \odot X = [M_1 X_1, \cdots, M_l X_l]. \tag{1}$$

To simplify the notation, we denote $f_g(X)$ as Z in the following sections, i.e., $f_g(X) = Z$.

We consider that X consists of a set of variables $\{T_1, \cdots, T_n, R\}$, where R denotes the real rationale (e.g., sentiment tendency for sentiment classification) for task label Y, and $T_1, \cdots, T_n$ are some **t**rivial patterns independent with Y. And we select one of $\{T_1, \cdots, T_n, R\}$ to be Z. Note that Z is not a separate variable but a proxy for any variable within X. Till now, we get a set of (Z,Y) samples denoted as $\mathcal{D}_\mathcal{Z}$. Previous research simply thinks $\mathcal{D}_\mathcal{Z}$ is collected from $P(Z,Y)$. By enumerating Z in $\mathcal{D}_\mathcal{Z}$, they get $P(Y|Z)$ and attempt to identify the rationale by maximizing the mutual information:

$$\begin{aligned} Z^* &= \underset{Z \in \{T_1,\cdots,T_n,R\}}{\arg\max} \; I(Y;Z) \\ &= \underset{Z \in \{T_1,\cdots,T_n,R\}}{\arg\max} \; (H(Y) - H(Y|Z)) \\ &= \underset{Z \in \{T_1,\cdots,T_n,R\}}{\arg\min} \; H(Y|Z). \end{aligned} \tag{2}$$

In practice, the entropy $H(Y|Z)$ is commonly approximated by the minimum cross-entropy $\min_{\theta_p} H_c(Y, \hat{Y}|Z)$, with $\hat{Y} = f_p(Z)$ representing the output of the predictor (note that the minimum cross-entropy is equal to the entropy, Appendix C.3). Replacing Z with $f_g(X)$, the generator and the predictor are trained cooperatively:

$$\min_{\theta_g, \theta_p} H_c(Y, f_p(f_g(X)) | f_g(X)), \; s.t., \; (X,Y) \sim \mathcal{D}. \tag{3}$$

Compactness and coherence. To make the rationales human-intelligible, previous methods usually constrains the rationales by compact and coherent regularization terms. We use the widely used constraints provided by Chang et al.

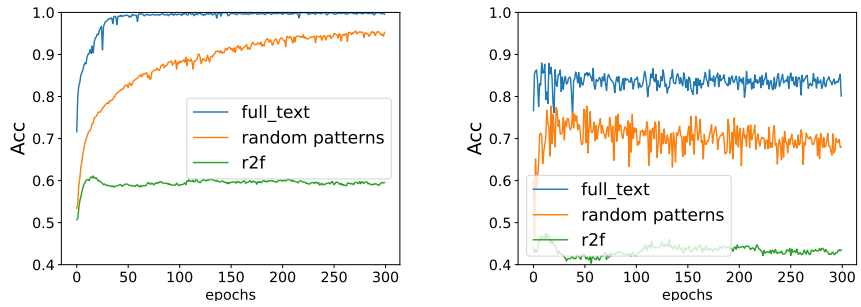

(a) Training (b) Validation

Figure 3. Experiments on the Beer-Aroma dataset (other datasets are in Appendix B.2): "full text": a predictor trained using the full texts. "random patterns": a predictor trained with randomly selected patterns. "r2f": feeding the random patterns to the predictor that was trained using the full texts.

(2019):

$$\Omega(M) = \lambda_1 \left| \frac{\|M\|_1}{l} - s \right| + \lambda_2 \sum_{t=2}^{l} \left| M_t - M_{t-1} \right|. \quad (4)$$

The first term encourages that the percentage of the tokens being selected as rationales is close to a pre-defined level s. The second term encourages the rationales to be coherent.

4. Motivation and method

Notation. For the sake of exposition, let us take the example of binary sentiment classification. We denote X^1 and X^0 as input texts with label $Y = 1$ and $Y = 0$, respectively. Z and Z_A represent the rationale candidates selected by the generator and the attacker, respectively. Note that they are not separate variables but a proxy for any variables within X. Sometimes we use Z and the variable represented by Z interchangeably. T is a proxy for any variables within $\{T_1, \cdots, T_n\}$ (defined in §3).

4.1. Cause of the spurious correlation

How do trivial patterns correlate with Y? Although considering $\mathcal{D}_Z$ as an approximation of $P(Z, Y)$ seems to be a simple and practical way and is inherited by all the previous methods (§3), it will sometimes results in some problems. In fact, the sampling process of Z is conditioned on a generator g with specific parameters θ_g. So we can only get $P(Z, Y|g)$ and $P(Y|Z, g)$ rather than $P(Z, Y)$ and $P(Y|Z)$. Note that independent doesn't lead to conditional independent: $Y \perp\!\!\!\perp Z \not\Rightarrow Y \perp\!\!\!\perp Z|g$. That is to say, some uninformative Z (like those $T_1, \cdots, T_n$) might initially be independent with Y and maintain zero mutual information with Y. But sampled by g, any trivial patterns may get correlated with Y and get increased mutual information, thus can be used as (incorrect) indicative features for classification.

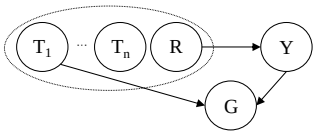

Figure 4. A local of the causal graph for the generator's updating process. Dash cycle means X consists of a set of variables.

What's more, the training process may even enhance the sampling bias further. For example, we consider T_1 is selected as Z, then the updating of the generator is $\theta'_g = h(\theta_g, T_1, Y)$ (h denotes the backpropagation process), and this structural function corresponds to a small local of a causal graph shown in Figure 4. We originally have $Y \perp\!\!\!\perp T_1$. But in this graph, we have $Y \not\perp\!\!\!\perp T_1|G$. That's to say, any trivial patterns hold the potential to be associated with Y through the influence of the generator.

Consider a situation where $Z = T$ is a trivial pattern independent with Y (i.e., $P(Y = 1|T) = P(Y = 1) = 0.5 = P(Y = 0) = P(Y = 0|T)$ and $T \in \{t_+, t_-\}$). Influenced by the generator g, $T = t_+$ might co-occur more frequently with $Y = 1$ and can be viewed as an indicator for the positive class ($T = t_-$ is similar):

$$\begin{cases} P(Y = 1|Z = t_+, g) > P(Y = 1) \\ P(Y = 0|Z = t_+, g) < P(Y = 0). \end{cases} \quad (5)$$

Example 1 in Figure 2 of §1 also provides an intuition for the above analysis.

Empirical support. The above motivation is inspired by some practical observations. We present three types of prediction accuracies for a binary sentiment classification task (about the beer's aroma) in Figure 3: ① A predictor trained with the full input text. ② A predictor trained with randomly selected patterns. For the generator, we remove the other objectives and only train it with the sparsity constraints (Equation 4). That is to say, the generator is trained to randomly select 10% of the input text, and the predictor is

then trained to classify using these randomly selected texts. ③ We use the randomly selected texts from ② to feed the predictor trained in ①.

From Figure 3(a), we observe that even with the randomly selected patterns (i.e., patterns unlikely to contain real rationales), the predictor can still achieve a very high prediction accuracy (represented by the orange line, approximately 95%). This accuracy is close to that of the classifier trained with the full texts. A follow-up question is: Does this strange result stem from the fact that the 10% randomly selected patterns already contain enough sentiment inclination for classification? The answer is no. Consider the green line, which represents the outcome when we feed the randomly selected texts to the well-trained predictor denoted by the blue line. We observe that the green line indicates a significantly lower accuracy (about 58%), implying that the randomly selected patterns contain only minimal sentiment information. Thus, the orange predictor incorrectly treats certain randomly selected trivial patterns as indicative features. Moreover, the orange predictor does not generalize well to the validation set (Figure 3(b)), due to the fact that simple trivial patterns can more easily lead to overfitting (Pagliardini et al., 2023).

We provide more evidence of the existence of such spurious correlations in practical scenarios from another perspective by demonstrating the attack success rate in §5.2.

4.2. The proposed method

For the sake of clarity, we first present our approach and then expound on the principles underlying it.

Figure 5 shows the architecture of our method. For a data point (X, Y) in a n-class classification task, the over all objective of our model (f_p, f_g, f_a represent the predictor, the generator, and the attacker, with $\theta_p, \theta_g, \theta_a$ being their parameters) is:

$$\textbf{attacker}: \min_{\theta_a} H_c(Y_A, f_p(f_a(X))|f_a(X)), \tag{6}$$

$$\begin{aligned}\textbf{gen\&pred}: &\min_{\theta_g,\theta_p} H_c(Y, f_p(f_g(X))|f_g(X)) \\ &+ \min_{\theta_p} H_c([1/n, \cdots, 1/n], f_p(f_a(X)|f_a(X))\end{aligned} \tag{7}$$

$$s.t.\ Y_A = \text{randint}(0, n) \& Y_A \neq Y. \tag{8}$$

Y_A represents the class to be attacked. We randomly select a class for each attack to create a balanced attack for each class. $[1/n, \cdots, 1/n]$ represents the distribution of $P(Y)$ in the raw dataset. $\min_{\theta_p} H_c([1/n, \cdots, 1/n], f_p(f_a(X)|f_a(X))$ means we rectify the sampled distribution of $P(Y|Z_A, a)$ to $P(Y)$ and ask the predictor to learn that Z_A is not correlated with Y. In binary classification, we have $Y_A = 1 - Y$ and $1/n = 0.5$.

During training, (7) and (6) are alternated. The practical implementation details with Pytorch are in Appendix A.3. The overall mechanism of the model is as follows: (6) inspects trivial patterns ($f_a(X)$) from X. The second term of (7) is the instruction that prevents the predictor from learning the trivial patterns by classifying them as random noise. A well instructed predictor is then able to give good feedback to the generator's selection. And the first term of (7) is the normal RNP. The reason why the attacker constructed in this manner can detect trivial patterns will be elucidated in §4.3. We also use a toy example in Appendix A.2 to provide an intuitive understanding. At the end of §4.3, we also discuss how our method will work in the situation where the generator and the predictor cooperate correctly on real rationales rather than trivial patterns.

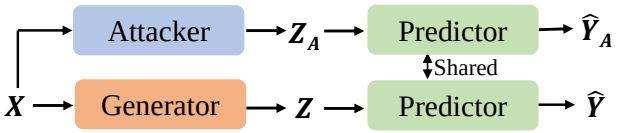

Figure 5. The architecture of attacking for inspection and instruction. We name it **A**ttack to **I**nspection and **I**nstruction (A2I). Z, Z_A represent the selected rationale candidate and the attack rationale. $\hat{Y}, \hat{Y}_A$ represent the normal prediction and the attack result.

4.3. Underlying principles

Attack as inspection. Following the above settings for $Z = T$ and $I(Y;T) = 0$ in §4.1, we will show how the trivial patterns learned by the predictor can be inspected through attack. Corresponding to (5), if the attack generator can be constructed in any way (i.e., has infinite expressiveness), then we can always find an attack generator g_a which extracts Z_A from X, such that

$$\begin{cases} P(Y=1|Z_A=t_+, g_a) < P(Y=1) \\ P(Y=0|Z_A=t_+, g_a) > P(Y=0). \end{cases} \tag{9}$$

Appendix C.1 shows the detailed derivation for the reason why we can find such a g_a. Equation (9) is the opposite of (5), and it means that under condition g_a, $T = t_+$ now becomes a negative class indicator, which is exactly the opposite situation under condition g. Here is the intuitive understanding of the attack. Corresponding to the punctuation pattern example mentioned in Figure 2 of §1. The generator g selects $Z =$ "." from X^1. And the predictor has learnt to predict "." as positive. We can employ an attacker g_a which selects $Z_A =$ "." from X^0 (whose class label is negative) such that Z_A can also be classified as positive. Similarly, the attacker can find $Z_A =$ "," from X^1 to be classified as negative. So, the overall objective of the attacker is to select those Z_A that can be classified to the opposite class by the predictor.

Table 1. Results on datasets from the BeerAdvocate benchmark. We follow Inter_RAT to set $S \approx 10\%, 20\%, 30\%$.

Methods \ Datasets		Beer-Appearance					Beer-Aroma					Beer-Palate				
		S	Acc	P	R	F1	S	Acc	P	R	F1	S	Acc	P	R	F1
Comparison with standard RNP																
$S \approx 10\%$	RNP	10.1	79.7	69.3	37.6	48.8	10.0	82.9	81.3	52.4	63.7	9.3	84.7	68.6	51.3	58.7
	RNP+A2I	10.8	82.8	78.3	45.8	**57.8**	9.8	86.3	86.0	54.3	**66.6**	10.9	86.6	66.3	58.2	**62.0**
$S \approx 20\%$	RNP	19.8	86.3	69.8	74.6	72.1	20.7	84.5	43.6	58.1	49.8	20.1	82.6	47.6	77.0	58.8
	RNP+A2I	20.0	87.7	73.3	79.4	**76.2**	19.5	85.4	49.0	61.4	**54.5**	19.4	86.6	49.0	76.4	**59.7**
$S \approx 30\%$	RNP	30.4	84.3	52.9	86.7	65.7	30.7	81.8	39.2	77.2	52.0	30.1	87.1	29.3	71.0	41.5
	RNP+A2I	29.9	85.2	59.3	95.9	**73.3**	27.8	87.3	44.5	79.3	**57.0**	30.5	87.1	30.8	75.5	**43.7**
Comparison with advanced variants																
$S \approx 10\%$	Inter_RAT	13.2	-	50.0	35.7	41.6	13.8	-	64.0	56.9	60.2	13.0	-	47.2	49.3	48.2
	NIR	10.6	78.1	77.0	44.3	56.2	10.3	86.1	74.9	49.7	59.8	11.5	84.0	48.1	44.4	46.2
	FR	11.0	82.2	68.0	40.5	50.8	9.4	86.7	85.3	51.5	64.2	9.4	84.5	70.1	52.8	60.2
	FR+A2I	11.3	84.6	76.0	46.5	**57.7**	10.0	86.9	85.7	54.8	**66.9**	9.7	84.8	71.4	55.8	**62.6**
$S \approx 20\%$	Inter_RAT	20.2	-	45.8	50.4	48.0	22.0	-	47.2	67.3	55.5	20.2	-	39.9	64.9	49.4
	NIR	20.3	81.9	70.3	77.2	73.6	19.1	87.7	61.2	75.2	67.5	19.9	83.9	37.3	59.6	45.9
	FR	19.7	87.7	77.7	82.8	80.2	20.5	90.5	61.1	80.3	69.4	19.8	86.0	42.1	67.0	51.7
	FR+A2I	19.8	88.7	80.0	85.6	**82.7**	19.4	89.7	64.2	80.0	**71.2**	19.2	86.0	44.2	68.2	**53.7**
$S \approx 30\%$	Inter_RAT	28.3	-	48.6	74.9	59.0	31.5	-	37.4	76.2	50.2	29.2	-	29.7	69.7	41.7
	NIR	29.6	84.9	59.8	95.5	73.6	30.0	82.3	38.4	73.9	50.5	29.7	84.1	22.8	54.5	32.2
	FR	30.0	90.9	58.5	94.6	72.3	31.0	83.2	40.0	79.4	53.2	29.3	84.8	28.5	67.2	40.1
	FR+A2I	28.8	89.7	61.3	95.3	**74.6**	30.9	83.2	41.4	82.2	**55.1**	29.1	85.1	31.6	73.8	**44.2**

Formally, the objective of the attacker is

$$\min_{\theta_a} H_c(1-Y, f_p(f_a(X))|f_a(X)). \tag{10}$$

Till now, we have demonstrated that an attacker can identify uninformative trivial patterns and classify them into the opposite class. Then we begin to instruct the predictor to not learn from the trivial patterns (whether the attacker will select real rationales is discussed at the end of this section).

Attack as instruction. When the spurious correlation occurs, the attacker g_a consistently chooses a Z_A that is a label-independent trivial pattern. For a competent predictor p that discerns the authentic rationale, Z_A resembles noise independent with Y, ensuring its classification remains random without any leanings to a specific label. Thus, we introduce an extra instruction to the predictor:

$$\begin{aligned} &\min_{\theta_p} H_c([0.5, 0.5], f_p(Z_A)), \\ &s.t.,\ Z_A = f_a(X),\ (X,Y) \sim \mathcal{D}. \end{aligned} \tag{11}$$

That is to say, although we cannot promise the independence between Z_A and Y under the generator's conditional sampling, we can make $Z_A \perp\!\!\!\perp \hat{Y}$ through the predictor's prediction.

The situation of a text X contains both positive and negative sentiments. Here we consider $Z = R$, which is the true rationale based on which the label Y is assigned to X. We denote $R = r_+, R = r_-$ as positive and negative indicators, respectively. The question we want to discuss now is, if the generator and the predictor cooperates well on real rationales, what will happen if X contains both positive and negative sentiments?

The first glance might be that, both the generator and the attacker choose the true (but opposite) sentiment rationales, thereby leading to the predictor in (7) being unable to make the right prediction. But in practice, the predictor can overcome this obstacle. Consider an intuitive assumption:

Assumption 4.1. The positive rationale r_+ appears more often in positive texts than in negative ones: $P(r_+|Y=1) \geq P(r_+|Y=0)$.

This assumption stems from that we can always find r_+ in X^1, but sometimes not in X^0. If Assumption 4.1 holds, we can easily prove (please refer to Appendix C.2) that the predictor in (7) will still converge to predict $f(r_+)$ as positive with a high confidence (≥ 0.75).

5. Experiments

5.1. Settings

Baselines. We compare our A2I with the standard RNP and several recent representative methods: Inter_RAT (Yue et al., 2023) and CR (Zhang et al., 2023) represent recent causal methods, and FR (Liu et al., 2022) and NIR (Storek et al., 2023) represent recent methods designed to deal with degeneration. All of them have been discussed in §2.

Datasets. We first follow FR to examine on three datasets from BeerAdvocate benchmark (McAuley et al., 2012):

Table 2. Results on datasets from the HotelReview benchmark. We follow FR to set $S \approx 10\%$. *: results from FR.

	Datasets / Methods	Hotel-Location					Hotel-Service					Hotel-Cleanliness				
		S	Acc	P	R	F1	S	Acc	P	R	F1	S	Acc	P	R	F1
Comparison with standard RNP																
$S \approx 10\%$	RNP*	8.8	97.5	46.2	48.2	47.1	11.0	97.5	34.2	32.9	33.5	10.5	96.0	29.1	34.6	31.6
	RNP+A2I	9.0	97.5	50.2	53.4	**51.7**	11.6	97.0	46.8	47.4	**47.1**	9.7	96.5	34.7	38.2	**36.4**
Comparison with advanced variants																
$S \approx 10\%$	Inter_RAT	11.0	-	34.7	44.8	39.1	12.5	-	35.4	39.1	37.2	9.6	-	33.4	36.7	34.9
	NIR	10.2	93.5	45.1	54.2	49.2	11.0	95.5	44.9	43.2	44.0	10.6	96.0	34.1	40.9	37.2
	FR*	9.0	93.5	55.5	58.9	57.1	11.5	94.5	44.8	44.7	44.8	11.0	96.0	34.9	43.4	38.7
	FR+A2I	9.9	94.0	53.2	62.1	**57.3**	11.5	97.0	47.7	47.7	**47.7**	10.8	95.5	35.9	43.7	**39.4**

Table 3. Results on graph datasets. "()": std. The sparsity of selected rationale is set to be close to the sparsity of ground truth.

Datasets / Methods	BA2Motifs					GOODMotif				
	S	Acc	P	R	F1	S	Acc	P	R	F1
Comparison with standard RNP										
RNP	20.3 (2.5)	95.2 (1.9)	36.5 (5.5)	36.5 (2.2)	36.4 (3.8)	31.3 (2.3)	62.1 (3.1)	41.8 (2.5)	44.8 (4.8)	43.2 (3.6)
RNP+A2I	20.5 (2.3)	95.2 (1.5)	39.7 (3.5)	40.5 (2.9)	**40.0** (2.5)	31.4 (2.1)	63.7 (2.6)	43.1 (1.8)	46.3 (3.4)	44.6 (2.5)
Comparison with advanced variants										
FR	20.5 (2.3)	96.4 (1.8)	39.3 (5.9)	40.0 (4.9)	39.6 (5.2)	32.8 (3.1)	64.5 (2.3)	41.9 (2.9)	47.1 (4.7)	44.3 (3.6)
FR+A2I	20.2 (1.5)	96.5 (1.4)	42.1 (2.8)	42.5 (4.0)	**42.3** (3.0)	32.5 (2.6)	66.5 (2.2)	43.8 (4.2)	48.8 (3.7)	46.1 (3.9)

Beer-Appearance, Beer-Aroma, Beer-Palate, and three datasets from HotelReview benchmark (Wang et al., 2010): Hotel-Location, Hotel-Service, Hotel-Cleanliness. Among them, the three beer-related datasets are used by nearly all of previous research in the field of rationalization. We also use two graph rationalization datasets, BA2Motifs (Ying et al., 2019) and GOODMotif (Gui et al., 2022), to verify generalizability. GOODMotif is a three-class graph classification dataset. These datasets include ground-truth rationales in their test sets to facilitate objective comparison between different methods. More details about the datasets are in Appendix A.4.

Metrics. Our findings suggest that even if the generator selects trivial patterns, the predictor can still get high final prediction accuracy. Thus the prediction performance is not a good metric for models' effectiveness. Following Inter_RAT and FR, we mainly focus on the rationale quality, which is measured by the overlap between model-selected tokens and human-annotated rationales. $P, R, F1$ denote precision, recall, and $F1$ score respectively. S (sparsity) represents the average percentage of selected tokens in relation to the full text. Acc stands for the predictive accuracy.

Details. The generator, predictor, and attacker all are composed of an encoder (RNN/Transformer/GNN) and a linear layer. We use three kinds of encoders: GRUs (following Inter_RAT and FR, Table 1 and 2), bert-base-uncased (following CR, Table 4), and GCN (for the BA2Motifs dataset). The random seed is kept the same (the seed is 12252018, inherited from the code of FR) across all the experiments on text classification, as we think experiments with multiple datasets and multiple sparsity settings (totally 12 settings in Table 1 and 2) under a unified seed are sufficient to verify that the improvements are not from randomness. The training of GNN is not as stable as GRUs, and we report the average results of five random seeds. More details are in Appendix A.5.

5.2. Results

Rationale quality. Table 1 and 2 show the results on the text classification datasets. For the most widely used beer-related datasets (which have been the most important benchmarks for a long time), we follow Inter_RAT to set three different sparsity levels: $10\%, 20\%, 30\%$, by adjusting s in Equation (4). For the hotel-related datasets, we use them as supplementary material and follow FR to set the sparisty to be similar to human-annotated rationales. Initially, we conduct our attacking inspection on top of the standard RNP to validate our claims and demonstrate the efficacy of our proposed method. Across all nine settings in Table 1, we observe a significant improvement over the standard RNP in terms of F1 score. Notably, the highest increase reaches up to 9.0% (*Beer-Appearance* with $S \approx 10\%$), underscoring the robust effectiveness of our method. Additionally, we compare with a representative LLM, llama-3.1-8b-instruct in Table 6 of Appendix D, and find that our simple A2I-based methods get comparable results to it and can sometimes even outperform it.

Our attack-based inspection is more of a tool than an independent model and is model-agnostic (as long as there is a predictor to attack). Therefore, we further apply it on top of the advanced method, FR (as FR outperforms Inter_RAT and NIR in most cases), to demonstrate our competitive-

Table 4. Results with BERT. We follow CR to set $S \approx 10\%$. "*": results obtained from CR.

Methods \ Datasets		Beer-Appearance			Beer-Aroma			Beer-Palate		
		P	R	F1	P	R	F1	P	R	F1
$S \approx 10\%$	RNP* (Lei et al., 2016)	48.7	11.7	20.0	44.2	20.7	27.6	25.1	21.9	22.8
	A2R* (Yu et al., 2021)	49.1	18.9	25.9	51.2	21.2	29.8	31.8	24.3	25.4
	CR* (Zhang et al., 2023)	45.3	22.0	28.0	60.3	35.4	39.0	32.5	25.9	26.5
	FR (Liu et al., 2022)	41.8	19.3	26.4	47.1	27.6	34.8	32.6	29.4	30.9
	FR+A2I	48.6	25.7	**33.6**	55.4	32.0	**40.5**	34.4	32.3	**33.3**

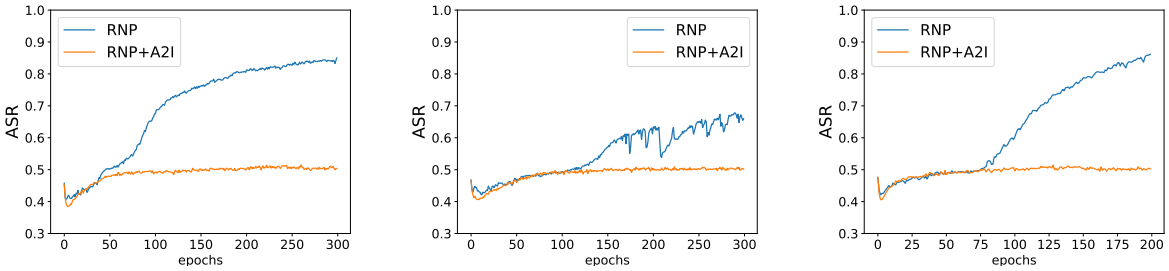

(a) Beer-Appearance (b) Beer-Aroma (c) Beer-Palate

Figure 6. Attack success rate on the three beer-related datasets. The rationale sparsity is about 20%. Results for sparsity being 10% and 30% are in Appendix B.1.

ness. Two observations emerge from the results. When our A2I is incorporated, the performance of both RNP and FR consistently improves. We observe a significant improvement in FR's performance (up to 6.9% on *Beer-Appearance* with $S \approx 10\%$) when our A2I is layered atop it, highlighting the competitiveness of our method. Aside from the most widely used beer-related datasets, we also consistently achieve strong performance on the hotel-related datasets (Table 2) and the graph datasets BA2Motifs and GOODMotif (Table 3) (note that Inter_RAT, NIR, and CR are methods specifically designed for text tasks and are not suitable for graph tasks).

Results with BERT. To show the competitiveness of A2I, we also follow CR to conduct experiments with pretrained BERT on the three most widely used beer-related datasets (Table 4) and compare with some methods that have already been implemented with BERT. We still get considerable improvements as compared to recent methods.

Attack Success Rate (ASR). To more effectively demonstrate the capabilities of our attacking inspection, we present the attack success rates for both RNP and our RNP+A2I. This experiment aims to address two key questions: 1) Can the attacker truly identify the trivial patterns recognized by the predictor? 2) Can the inspection really prevent the predictor from adopting the trivial patterns? ASR is a metric commonly employed in the realm of security. Given a pair (X, Y), if $f_p(f_a(X)) = 1 - Y$, indicating a label inversion, we deem the attack successful. ASR serves as an indicator of both an attack method's efficacy and a model's resilience against such attacks. A high ASR signifies the effectiveness of an attack method, while a low ASR denotes model robustness. The results for the three beer-related datasets are displayed in Figure 6. Regarding the first question, "Can the attacker truly identify the trivial patterns learned by the predictor?", the blue lines offer insight. As opposed to RNP+A2I, the blue lines depict models where we omit the objective Equation (11) (specifically, the instruction loss) from Equation (7). This means that while RNP is trained as usual, an attacker is also being trained concurrently. The prominence of the blue lines demonstrates that the attacker achieves a remarkably high ASR. This indicates that the predictor in RNP does internalize some trivial patterns, and the attacker successfully identifies them, underscoring the potency of the attack. For the second question, "Can the inspection effectively deter the predictor from adopting trivial patterns?", we can look to the orange lines. The ASR values hover around 50%, which is close to random classification. This suggests that the attacker can only select some neutral patterns and the predictor actively avoids learning from the trivial patterns, highlighting the efficacy of the instruction.

6. Conclusion

This paper investigates a new type of spurious correlation (i.e., model-added spurious correlation) in the self-explaining rationalization framework. It can appear even in clean datasets, thus making previous causal methods (which

focus solely on the causal relationships in the raw dataset) ineffective in dealing with it. We design an attack-based method to inspect the model-added spurious correlations and to instruct the training of rationalization. Experiments on both text and graph domains show the effectiveness of the proposed method.

Impact Statement

This paper aims to investigate the interpretability of machine learning models. In our view, our research is unlikely to produce negative social impacts.

Exploring XAI techniques can help to address many important problems existed in present deep learning models. For instance, XAI techniques can aid in detecting model discrimination (fairness) (Pradhan et al., 2022) or jailbreaks (Jiang et al., 2025), identifying backdoor attacks (security) (Yu et al., 2025a;b; Yang et al., 2025), controlling robots (Zhou et al., 2025), and revealing potential spurious correlations (robustness) (Yang et al., 2024), among others. Another direction is how to apply the findings of this direction into other modalities (Diao et al., 2024; 2025; Bi et al., 2025b;a).

Acknowledgements

This work is supported by the National Key Research and Development Program of China under grant 2024YFC3307900; the National Natural Science Foundation of China under grants 62376103, 62302184, 62436003 and 62206102; Major Science and Technology Project of Hubei Province under grant 2024BAA008; Hubei Science and Technology Talent Service Project under grant 2024DJC078; and Ant Group through CCF-Ant Research Fund. The computation is completed in the HPC Platform of Huazhong University of Science and Technology.

We sincerely thank the reviewers for their valuable feedback and efforts during the review process. They have helped a lot in improving the quality of this paper. We thank Yuankai Zhang for providing additional results on other baselines.

References

Bao, Y., Chang, S., Yu, M., and Barzilay, R. Deriving machine attention from human rationales. In *Proceedings of the 2018 Conference on Empirical Methods in Natural Language Processing, Brussels, Belgium, October 31 - November 4, 2018*, pp. 1903–1913. Association for Computational Linguistics, 2018. doi: 10.18653/v1/d18-1216. URL https://doi.org/10.18653/v1/d18-1216.

Bastings, J., Aziz, W., and Titov, I. Interpretable neural predictions with differentiable binary variables. In *Proceedings of the 57th Conference of the Association for Computational Linguistics, ACL 2019, Florence, Italy, July 28- August 2, 2019, Volume 1: Long Papers*, pp. 2963–2977. Association for Computational Linguistics, 2019. doi: 10.18653/v1/p19-1284. URL https://doi.org/10.18653/v1/p19-1284.

Bi, J., Wang, Y., Chen, H., Xiao, X., Hecker, A., Tresp, V., and Ma, Y. Llava steering: Visual instruction tuning with 500x fewer parameters through modality linear representation-steering, 2024. URL https://arxiv.org/abs/2412.12359.

Bi, J., Wang, Y., Yan, D., Xiao, X., Hecker, A., Tresp, V., and Ma, Y. Prism: Self-pruning intrinsic selection method for training-free multimodal data selection. *arXiv preprint arXiv:2502.12119*, 2025a.

Bi, J., Yan, D., Wang, Y., Huang, W., Chen, H., Wan, G., Ye, M., Xiao, X., Schuetze, H., Tresp, V., et al. Cot-kinetics: A theoretical modeling assessing lrm reasoning process. *arXiv preprint arXiv:2505.13408*, 2025b.

Chan, A., Sanjabi, M., Mathias, L., Tan, L., Nie, S., Peng, X., Ren, X., and Firooz, H. UNIREX: A unified learning framework for language model rationale extraction. In *International Conference on Machine Learning, ICML 2022, 17-23 July 2022, Baltimore, Maryland, USA*, volume 162 of *Proceedings of Machine Learning Research*, pp. 2867–2889. PMLR, 2022. URL https://proceedings.mlr.press/v162/chan22a.html.

Chang, S., Zhang, Y., Yu, M., and Jaakkola, T. S. A game theoretic approach to class-wise selective rationalization. In *Advances in Neural Information Processing Systems 32: Annual Conference on Neural Information Processing Systems 2019, NeurIPS 2019, December 8-14, 2019, Vancouver, BC, Canada*, pp. 10055–10065, 2019.

Chang, S., Zhang, Y., Yu, M., and Jaakkola, T. S. Invariant rationalization. In *Proceedings of the 37th International Conference on Machine Learning, ICML 2020, 13-18 July 2020, Virtual Event*, volume 119 of *Proceedings of Machine Learning Research*, pp. 1448–1458. PMLR, 2020. URL http://proceedings.mlr.press/v119/chang20c.html.

Chen, H., He, J., Narasimhan, K., and Chen, D. Can rationalization improve robustness? In *Proceedings of the 2022 Conference of the North American Chapter of the Association for Computational Linguistics: Human Language Technologies, NAACL 2022, Seattle, WA, United States, July 10-15, 2022*, pp. 3792–3805. Association for Computational Linguistics, 2022. doi: 10.18653/v1/2022.naacl-main.278. URL https://doi.org/10.18653/v1/2022.naacl-main.278.

Cho, K., van Merrienboer, B., Gülçehre, Ç., Bahdanau, D., Bougares, F., Schwenk, H., and Bengio, Y. Learning phrase representations using RNN encoder-decoder for statistical machine translation. In *Proceedings of the 2014 Conference on Empirical Methods in Natural Language Processing, EMNLP 2014, October 25-29, 2014, Doha, Qatar, A meeting of SIGDAT, a Special Interest Group of the ACL*, pp. 1724–1734. ACL, 2014. doi: 10.3115/v1/d14-1179. URL https://doi.org/10.3115/v1/d14-1179.

Cui, W., Jiao, X., Meng, Z., and King, I. Voxeval: Benchmarking the knowledge understanding capabilities of end-to-end spoken language models. In Che, W., Nabende, J., Shutova, E., and Pilehvar, M. T. (eds.), *Proceedings of the 63rd Annual Meeting of the Association for Computational Linguistics (Volume 1: Long Papers), ACL 2025, Vienna, Austria, July 27 - August 1, 2025*, pp. 16735–16753. Association for Computational Linguistics, 2025. URL https://aclanthology.org/2025.acl-long.818/.

Devlin, J., Chang, M., Lee, K., and Toutanova, K. BERT: pre-training of deep bidirectional transformers for language understanding. In *Proceedings of the 2019 Conference of the North American Chapter of the Association for Computational Linguistics: Human Language Technologies, NAACL-HLT 2019, Minneapolis, MN, USA, June 2-7, 2019, Volume 1 (Long and Short Papers)*, pp. 4171–4186. Association for Computational Linguistics, 2019. doi: 10.18653/v1/n19-1423. URL https://doi.org/10.18653/v1/n19-1423.

DeYoung, J., Jain, S., Rajani, N. F., Lehman, E., Xiong, C., Socher, R., and Wallace, B. C. ERASER: A benchmark to evaluate rationalized NLP models. In *Proceedings of the 58th Annual Meeting of the Association for Computational Linguistics*, pp. 4443–4458, Online, July 2020. Association for Computational Linguistics. doi: 10.18653/v1/2020.acl-main.408. URL https://aclanthology.org/2020.acl-main.408.

Diao, X., Zhang, C., Wu, T., Cheng, M., Ouyang, Z., Wu, W., and Gui, J. Learning musical representations for music performance question answering. In *Findings of the Association for Computational Linguistics: EMNLP 2024*, 2024.

Diao, X., Zhang, C., Wu, W., Ouyang, Z., Qing, P., Cheng, M., Vosoughi, S., and Gui, J. Temporal working memory: Query-guided segment refinement for enhanced multimodal understanding. In *Findings of the Association for Computational Linguistics: NAACL 2025*, 2025.

Ghassemi, M., Oakden-Rayner, L., and Beam, A. L. The false hope of current approaches to explainable artificial intelligence in health care. *The Lancet Digital Health*, 3 (11):e745–e750, 2021.

Gui, S., Li, X., Wang, L., and Ji, S. GOOD: A graph out-of-distribution benchmark. In *Advances in Neural Information Processing Systems 35: Annual Conference on Neural Information Processing Systems 2022, NeurIPS 2022, New Orleans, LA, USA, November 28 - December 9, 2022*, 2022.

Gui, S., Liu, M., Li, X., Luo, Y., and Ji, S. Joint learning of label and environment causal independence for graph out-of-distribution generalization. *arXiv preprint arXiv:2306.01103*, 2023.

Guo, Z., Jin, R., Liu, C., Huang, Y., Shi, D., Supryadi, Yu, L., Liu, Y., Li, J., Xiong, B., and Xiong, D. Evaluating large language models: A comprehensive survey. *CoRR*, abs/2310.19736, 2023. doi: 10.48550/ARXIV.2310.19736. URL https://doi.org/10.48550/arXiv.2310.19736.

Hase, P., Zhang, S., Xie, H., and Bansal, M. Leakage-adjusted simulatability: Can models generate non-trivial explanations of their behavior in natural language? In *Findings of the Association for Computational Linguistics: EMNLP 2020*, pp. 4351–4367, 2020.

Huang, Y., Chen, Y., Du, Y., and Yang, Z. Distribution matching for rationalization. In *Thirty-Fifth AAAI Conference on Artificial Intelligence, AAAI 2021, Thirty-Third Conference on Innovative Applications of Artificial Intelligence, IAAI 2021, The Eleventh Symposium on Educational Advances in Artificial Intelligence, EAAI 2021, Virtual Event, February 2-9, 2021*, pp. 13090–13097. AAAI Press, 2021. URL https://ojs.aaai.org/index.php/AAAI/article/view/17547.

Jacovi, A. and Goldberg, Y. Towards faithfully interpretable NLP systems: How should we define and evaluate faithfulness? In *Proceedings of the 58th Annual Meeting of the Association for Computational Linguistics, ACL 2020, Online, July 5-10, 2020*, pp. 4198–4205. Association for Computational Linguistics, 2020. doi: 10.18653/V1/2020.ACL-MAIN.386. URL https://doi.org/10.18653/v1/2020.acl-main.386.

Jacovi, A. and Goldberg, Y. Aligning faithful interpretations with their social attribution. *Transactions of the Association for Computational Linguistics*, 9:294–310, 2021. doi: 10.1162/tacl_a_00367. URL https://aclanthology.org/2021.tacl-1.18.

Jain, S., Wiegreffe, S., Pinter, Y., and Wallace, B. C. Learning to faithfully rationalize by construction. In *Proceedings of the 58th Annual Meeting of the Association for Computational Linguistics, ACL 2020, Online, July 5-10, 2020*, pp. 4459–4473. Association for

Computational Linguistics, 2020. doi: 10.18653/v1/2020.acl-main.409. URL https://doi.org/10.18653/v1/2020.acl-main.409.

Jang, E., Gu, S., and Poole, B. Categorical reparameterization with gumbel-softmax. In *5th International Conference on Learning Representations, ICLR 2017, Toulon, France, April 24-26, 2017, Conference Track Proceedings*. OpenReview.net, 2017. URL https://openreview.net/forum?id=rkE3y85ee.

Jiang, Y., Gao, X., Peng, T., Tan, Y., Zhu, X., Zheng, B., and Yue, X. Hiddendetect: Detecting jailbreak attacks against large vision-language models via monitoring hidden states, 2025. URL https://arxiv.org/abs/2502.14744.

Kingma, D. P. and Ba, J. Adam: A method for stochastic optimization. In *3rd International Conference on Learning Representations, ICLR 2015, San Diego, CA, USA, May 7-9, 2015, Conference Track Proceedings*, 2015. URL http://arxiv.org/abs/1412.6980.

Lei, T., Barzilay, R., and Jaakkola, T. S. Rationalizing neural predictions. In *Proceedings of the 2016 Conference on Empirical Methods in Natural Language Processing, EMNLP 2016, Austin, Texas, USA, November 1-4, 2016*, pp. 107–117. The Association for Computational Linguistics, 2016. doi: 10.18653/v1/d16-1011. URL https://doi.org/10.18653/v1/d16-1011.

Lipton, Z. C. The mythos of model interpretability: In machine learning, the concept of interpretability is both important and slippery. *Queue*, 16(3):31–57, 2018.

Liu, W., Wang, H., Wang, J., Li, R., Yue, C., and Zhang, Y. FR: Folded rationalization with a unified encoder. In *Advances in Neural Information Processing Systems*, 2022. URL https://openreview.net/forum?id=ZPyKSBaKkiO.

Liu, W., Wang, H., Wang, J., Li, R., Li, X., Zhang, Y., and Qiu, Y. MGR: multi-generator based rationalization. In Rogers, A., Boyd-Graber, J. L., and Okazaki, N. (eds.), *Proceedings of the 61st Annual Meeting of the Association for Computational Linguistics (Volume 1: Long Papers), ACL 2023, Toronto, Canada, July 9-14, 2023*, pp. 12771–12787. Association for Computational Linguistics, 2023a. doi: 10.18653/v1/2023.acl-long.715. URL https://doi.org/10.18653/v1/2023.acl-long.715.

Liu, W., Wang, J., Wang, H., Li, R., Deng, Z., Zhang, Y., and Qiu, Y. D-separation for causal self-explanation. In *Advances in Neural Information Processing Systems 36: Annual Conference on Neural Information Processing Systems 2023, NeurIPS 2023, New Orleans, LA, USA, December 10 - 16, 2023*, 2023b.

Liu, W., Wang, J., Wang, H., Li, R., Qiu, Y., Zhang, Y., Han, J., and Zou, Y. Decoupled rationalization with asymmetric learning rates: A flexible lipschitz restraint. In *Proceedings of the 29th ACM SIGKDD Conference on Knowledge Discovery and Data Mining, KDD 2023, Long Beach, CA, USA, August 6-10, 2023*, pp. 1535–1547. ACM, 2023c. doi: 10.1145/3580305.3599299. URL https://doi.org/10.1145/3580305.3599299.

Liu, W., Deng, Z., Niu, Z., Wang, J., Wang, H., Zhang, Y., and Li, R. Is the mmi criterion necessary for interpretability? degenerating non-causal features to plain noise for self-rationalization. In *The Thirty-eighth Annual Conference on Neural Information Processing Systems*, 2024a.

Liu, W., Wang, H., Wang, J., Deng, Z., Zhang, Y., Wang, C., and Li, R. Enhancing the rationale-input alignment for self-explaining rationalization. In *40th IEEE International Conference on Data Engineering, ICDE 2024, Utrecht, The Netherlands, May 13-16, 2024*, pp. 2218–2230. IEEE, 2024b. doi: 10.1109/ICDE60146.2024.00176. URL https://doi.org/10.1109/ICDE60146.2024.00176.

Liu, W., Deng, Z., Niu, Z., Wang, J., Wang, H., Zeng, Z., and Li, R. Breaking free from MMI: A new frontier in rationalization by probing input utilization. In *The Thirteenth International Conference on Learning Representations*, 2025. URL https://openreview.net/forum?id=WZ0s2smcKP.

Luo, D., Cheng, W., Xu, D., Yu, W., Zong, B., Chen, H., and Zhang, X. Parameterized explainer for graph neural network. In *Advances in Neural Information Processing Systems 33: Annual Conference on Neural Information Processing Systems 2020, NeurIPS 2020, December 6-12, 2020, virtual*, 2020.

McAuley, J. J., Leskovec, J., and Jurafsky, D. Learning attitudes and attributes from multi-aspect reviews. In *12th IEEE International Conference on Data Mining, ICDM 2012, Brussels, Belgium, December 10-13, 2012*, pp. 1020–1025. IEEE Computer Society, 2012. doi: 10.1109/ICDM.2012.110. URL https://doi.org/10.1109/ICDM.2012.110.

Pagliardini, M., Jaggi, M., Fleuret, F., and Karimireddy, S. P. Agree to disagree: Diversity through disagreement for better transferability. In *The Eleventh International Conference on Learning Representations, ICLR 2023, Kigali, Rwanda, May 1-5, 2023*. OpenReview.net, 2023. URL https://openreview.net/pdf?id=K7CbYQbyYhY.

Paranjape, B., Joshi, M., Thickstun, J., Hajishirzi, H., and Zettlemoyer, L. An information bottleneck approach

for controlling conciseness in rationale extraction. In *Proceedings of the 2020 Conference on Empirical Methods in Natural Language Processing, EMNLP 2020, Online, November 16-20, 2020*, pp. 1938–1952. Association for Computational Linguistics, 2020. doi: 10.18653/v1/2020.emnlp-main.153. URL https://doi.org/10.18653/v1/2020.emnlp-main.153.

Pennington, J., Socher, R., and Manning, C. D. Glove: Global vectors for word representation. In *Proceedings of the 2014 Conference on Empirical Methods in Natural Language Processing, EMNLP 2014, October 25-29, 2014, Doha, Qatar, A meeting of SIGDAT, a Special Interest Group of the ACL*, pp. 1532–1543. ACL, 2014. doi: 10.3115/v1/d14-1162. URL https://doi.org/10.3115/v1/d14-1162.

Plyler, M., Green, M., and Chi, M. Making a (counterfactual) difference one rationale at a time. In *Advances in Neural Information Processing Systems 34: Annual Conference on Neural Information Processing Systems 2021, NeurIPS 2021, December 6-14, 2021, virtual*, pp. 28701–28713, 2021.

Pradhan, R., Zhu, J., Glavic, B., and Salimi, B. Interpretable data-based explanations for fairness debugging. In *SIGMOD '22: International Conference on Management of Data, Philadelphia, PA, USA, June 12 - 17, 2022*, pp. 247–261. ACM, 2022. doi: 10.1145/3514221.3517886. URL https://doi.org/10.1145/3514221.3517886.

Rajagopal, D., Balachandran, V., Hovy, E. H., and Tsvetkov, Y. SELFEXPLAIN: A self-explaining architecture for neural text classifiers. In *Proceedings of the 2021 Conference on Empirical Methods in Natural Language Processing*, pp. 836–850, Online and Punta Cana, Dominican Republic, November 2021. Association for Computational Linguistics. doi: 10.18653/v1/2021.emnlp-main.64. URL https://aclanthology.org/2021.emnlp-main.64.

Ren, Q., Gao, J., Shen, W., and Zhang, Q. Where we have arrived in proving the emergence of sparse interaction primitives in DNNs. In *The Twelfth International Conference on Learning Representations*, 2024. URL https://openreview.net/forum?id=3pWSL8My6B.

Rudin, C. Stop explaining black box machine learning models for high stakes decisions and use interpretable models instead. *Nature Machine Intelligence*, 1(5):206–215, 2019. doi: 10.1038/S42256-019-0048-X. URL https://doi.org/10.1038/s42256-019-0048-x.

Seiler, B. B. *Applications of Cooperative Game Theory to Interpretable Machine Learning*. PhD thesis, Stanford University, 2023.

Sha, L., Camburu, O., and Lukasiewicz, T. Learning from the best: Rationalizing predictions by adversarial information calibration. In *Thirty-Fifth AAAI Conference on Artificial Intelligence, AAAI 2021, Thirty-Third Conference on Innovative Applications of Artificial Intelligence, IAAI 2021, The Eleventh Symposium on Educational Advances in Artificial Intelligence, EAAI 2021, Virtual Event, February 2-9, 2021*, pp. 13771–13779. AAAI Press, 2021. URL https://ojs.aaai.org/index.php/AAAI/article/view/17623.

Storek, A., Subbiah, M., and McKeown, K. R. Unsupervised selective rationalization with noise injection. In *Proceedings of the 61st Annual Meeting of the Association for Computational Linguistics (Volume 1: Long Papers), ACL 2023, Toronto, Canada, July 9-14, 2023*, pp. 12647–12659. Association for Computational Linguistics, 2023. doi: 10.18653/v1/2023.acl-long.707. URL https://doi.org/10.18653/v1/2023.acl-long.707.

Sun, L., Huang, Y., Wang, H., Wu, S., Zhang, Q., Gao, C., Huang, Y., Lyu, W., Zhang, Y., Li, X., Liu, Z., Liu, Y., Wang, Y., Zhang, Z., Kailkhura, B., Xiong, C., Zhang, C., Xiao, C., Li, C., Xing, E. P., Huang, F., Liu, H., Ji, H., Wang, H., Zhang, H., Yao, H., Kellis, M., Zitnik, M., Jiang, M., Bansal, M., Zou, J., Pei, J., Liu, J., Gao, J., Han, J., Zhao, J., Tang, J., Wang, J., Mitchell, J., Shu, K., Xu, K., Chang, K., He, L., Huang, L., Backes, M., Gong, N. Z., Yu, P. S., Chen, P., Gu, Q., Xu, R., Ying, R., Ji, S., Jana, S., Chen, T., Liu, T., Zhou, T., Wang, W., Li, X., Zhang, X., Wang, X., Xie, X., Chen, X., Wang, X., Liu, Y., Ye, Y., Cao, Y., and Zhao, Y. Trustllm: Trustworthiness in large language models. *CoRR*, abs/2401.05561, 2024a. doi: 10.48550/ARXIV.2401.05561. URL https://doi.org/10.48550/arXiv.2401.05561.

Sun, R., Zheng, Z., and Wang, Z. Learning encodings for constructive neural combinatorial optimization needs to regret. In *Proceedings of the AAAI Conference on Artificial Intelligence*, volume 38, pp. 20803–20811, 2024b.

Tong, J., Zhou, H., Liu, Y., Hu, Y., and Zou, Y. Dynamic knowledge adapter with probabilistic calibration for generalized few-shot semantic segmentation. In *Proceedings of the IEEE/CVF Conference on Computer Vision and Pattern Recognition*, pp. 2781–2790, 2024a.

Tong, J., Zou, Y., Li, Y., and Li, R. Lightweight frequency masker for cross-domain few-shot semantic segmentation. *Advances in Neural Information Processing Systems*, 37: 96728–96749, 2024b.

Tong, J., Jin, W., Qin, P., Li, A., Zou, Y., Li, Y., Li, Y., and Li, R. Flowcut: Rethinking redundancy via information flow for efficient vision-language models. *arXiv preprint arXiv:2505.19536*, 2025a.

Tong, J., Ma, R., Zou, Y., Chen, G., Li, Y., and Li, R. Adapter naturally serves as decoupler for cross-domain few-shot semantic segmentation. *arXiv preprint arXiv:2506.07376*, 2025b.

Wang, H., Lu, Y., and Zhai, C. Latent aspect rating analysis on review text data: a rating regression approach. In *Proceedings of the 16th ACM SIGKDD International Conference on Knowledge Discovery and Data Mining, Washington, DC, USA, July 25-28, 2010*, pp. 783–792. ACM, 2010. doi: 10.1145/1835804.1835903. URL https://doi.org/10.1145/1835804.1835903.

Wang, Q., Meng, Z., Cui, W., Zhang, Y., Wu, P., Wu, B., King, I., Chen, L., and Zhao, P. NTPP: generative speech language modeling for dual-channel spoken dialogue via next-token-pair prediction. *CoRR*, abs/2506.00975, 2025. doi: 10.48550/ARXIV.2506.00975. URL https://doi.org/10.48550/arXiv.2506.00975.

Wu, Y., Wang, X., Zhang, A., He, X., and Chua, T. Discovering invariant rationales for graph neural networks. In *The Tenth International Conference on Learning Representations, ICLR 2022, Virtual Event, April 25-29, 2022*. OpenReview.net, 2022. URL https://openreview.net/forum?id=hGXij5rfiHw.

Xia, M., Malladi, S., Gururangan, S., Arora, S., and Chen, D. LESS: selecting influential data for targeted instruction tuning. *CoRR*, abs/2402.04333, 2024. doi: 10.48550/ARXIV.2402.04333. URL https://doi.org/10.48550/arXiv.2402.04333.

Yang, J., Tang, A., Zhu, D., Chen, Z., Shen, L., and Wu, F. Mitigating the backdoor effect for multi-task model merging via safety-aware subspace. *arXiv preprint arXiv:2410.13910*, 2024.

Yang, J., Chen, Z., Xiao, T., Lin, Y., Zhang, W., and Kuang, K. Leveraging invariant principle for heterophilic graph structure distribution shifts. In *Proceedings of the ACM on Web Conference 2025*, pp. 1196–1204, 2025.

Ying, Z., Bourgeois, D., You, J., Zitnik, M., and Leskovec, J. Gnnexplainer: Generating explanations for graph neural networks. In *Advances in Neural Information Processing Systems 32: Annual Conference on Neural Information Processing Systems 2019, NeurIPS 2019, December 8-14, 2019, Vancouver, BC, Canada*, pp. 9240–9251, 2019.

Yu, M., Chang, S., Zhang, Y., and Jaakkola, T. S. Rethinking cooperative rationalization: Introspective extraction and complement control. In *Proceedings of the 2019 Conference on Empirical Methods in Natural Language Processing and the 9th International Joint Conference on Natural Language Processing, EMNLP-IJCNLP 2019, Hong Kong, China, November 3-7, 2019*, pp. 4092–4101. Association for Computational Linguistics, 2019. doi: 10.18653/v1/D19-1420. URL https://doi.org/10.18653/v1/D19-1420.

Yu, M., Zhang, Y., Chang, S., and Jaakkola, T. S. Understanding interlocking dynamics of cooperative rationalization. In *Advances in Neural Information Processing Systems 34: Annual Conference on Neural Information Processing Systems 2021, NeurIPS 2021, December 6-14, 2021, virtual*, pp. 12822–12835, 2021.

Yu, Y., Wang, Y., Yang, W., Guo, L., Lu, S., Duan, L., Tan, Y., and Kot, A. C. Robust and transferable backdoor attacks against deep image compression with selective frequency prior. *IEEE Trans. Pattern Anal. Mach. Intell.*, 47(3):1674–1693, 2025a. doi: 10.1109/TPAMI.2024.3507873. URL https://doi.org/10.1109/TPAMI.2024.3507873.

Yu, Y., Xia, S., Lin, X., Yang, W., Lu, S., Tan, Y., and Kot, A. C. Backdoor attacks against no-reference image quality assessment models via a scalable trigger. In Walsh, T., Shah, J., and Kolter, Z. (eds.), *AAAI-25, Sponsored by the Association for the Advancement of Artificial Intelligence, February 25 - March 4, 2025, Philadelphia, PA, USA*, pp. 9698–9706. AAAI Press, 2025b. doi: 10.1609/AAAI.V39I9.33051. URL https://doi.org/10.1609/aaai.v39i9.33051.

Yuan, H., Cai, L., Hu, X., Wang, J., and Ji, S. Interpreting image classifiers by generating discrete masks. *IEEE Trans. Pattern Anal. Mach. Intell.*, 44(4):2019–2030, 2022. doi: 10.1109/TPAMI.2020.3028783. URL https://doi.org/10.1109/TPAMI.2020.3028783.

Yue, L., Liu, Q., Wang, L., An, Y., Du, Y., and Huang, Z. Interventional rationalization. In *Proceedings of the 2016 Conference on Empirical Methods in Natural Language Processing, EMNLP 2023, Singapore, December 6–10, 2023*, 2023. URL https://openreview.net/forum?id=KoEa6h1o6D1.

Zhang, W., Wu, T., Wang, Y., Cai, Y., and Cai, H. Towards trustworthy explanation: On causal rationalization. In *Proceedings of the 40th International Conference on Machine Learning (ICML'23)*, volume 202 of *Proceedings of Machine Learning Research*, pp. 41715–41736. PMLR, 23–29 Jul 2023. URL https://arxiv.org/abs/2306.14115.

Zhao, W. X., Zhou, K., Li, J., Tang, T., Wang, X., Hou, Y., Min, Y., Zhang, B., Zhang, J., Dong, Z., Du, Y., Yang, C., Chen, Y., Chen, Z., Jiang, J., Ren, R., Li, Y., Tang, X., Liu, Z., Liu, P., Nie, J., and Wen, J. A survey of large language models. *CoRR*, abs/2303.18223, 2023. doi: 10.48550/ARXIV.2303.18223. URL https://doi.org/10.48550/arXiv.2303.18223.

Zheng, Y., Booth, S., Shah, J., and Zhou, Y. The irrationality of neural rationale models. In *Proceedings of the 2nd Workshop on Trustworthy Natural Language Processing (TrustNLP 2022)*, pp. 64–73, Seattle, U.S.A., July 2022. Association for Computational Linguistics. doi: 10.18653/v1/2022.trustnlp-1.6. URL https://aclanthology.org/2022.trustnlp-1.6.

Zheng, Z. and Lee, W. S. Reasoning-cv: Fine-tuning powerful reasoning llms for knowledge-assisted claim verification. *arXiv preprint arXiv:2505.12348*, 2025.

Zheng, Z., Yao, S., Li, G., Han, L., and Wang, Z. Pareto improver: Learning improvement heuristics for multi-objective route planning. *IEEE Transactions on Intelligent Transportation Systems*, 25(1):1033–1043, 2023.

Zheng, Z., Yao, S., Wang, Z., Tong, X., Yuan, M., and Tang, K. Dpn: Decoupling partition and navigation for neural solvers of min-max vehicle routing problems. *arXiv preprint arXiv:2405.17272*, 2024a.

Zheng, Z., Zhou, C., Xialiang, T., Yuan, M., and Wang, Z. Udc: A unified neural divide-and-conquer framework for large-scale combinatorial optimization problems. *Advances in Neural Information Processing Systems*, 37: 6081–6125, 2024b.

Zheng, Z., Xie, Z., Wang, Z., and Hooi, B. Monte carlo tree search for comprehensive exploration in llm-based automatic heuristic design. *arXiv preprint arXiv:2501.08603*, 2025.

Zhou, C., Jiang, R., Luan, F., Meng, S., Wang, Z., Dong, Y., Zhou, Y., and He, B. Dual-arm robotic fabric manipulation with quasi-static and dynamic primitives for rapid garment flattening. *IEEE/ASME Transactions on Mechatronics*, pp. 1–11, 2025. doi: 10.1109/TMECH.2025.3556283.

A. Eaxamples and implementations details

A.1. The potential impact of rationalization in the era of LLMs

In comparison to traditional "model-centric" XAI methods which solely focus on the model's learned information, "data-centric" approaches primarily aim to extract model-agnostic patterns inherent in the data. So, apart from improving interpretability, rationalization can serve as a method of data cleaning (Seiler, 2023).

Domain-specific large models often require supervised fine-tuning using domain-specific data. Uncleaned data may contain harmful information such as biases and stereotypes (Sun et al., 2024a). Recent research suggests that training predictors with extracted rationales can remove irrelevant harmful information, enhancing robustness (Chen et al., 2022) and generalization (Wu et al., 2022; Gui et al., 2023).

Since LLMs are usually pretrained on various datasets, they tend to be less controllable than small models (Zhao et al., 2023). Considering that for simple tasks (such as text classification), small models are also capable and can achieve satisfactory results, we can train a separate rationalization model for a single domain-specific dataset. Small models trained on a single dataset are often more controllable and save computational resources (such as searching for hyper-parameters and adding regularization terms) (Guo et al., 2023). Then using the extracted rationales for supervised fine-tuning might prevent large models from learning harmful information from new data. Additionally, shortening input texts can also reduce the memory required for fine-tuning.

Some recent studies has also found that training a small model for data selection (although not the same as rationale selection) and producing a small subset is useful for fine-tuning LLMs (Xia et al., 2024; Bi et al., 2024).

A.2. A toy example for a more intuitive understanding of the proposed method

Firstly, to inspect and identify the correlations, we introduce an attack generator g_a. Figure 7 shows an example of how the attacker works (formal analysis is in §4.3).

Example 2: the optimization objective of g_a is to select an attack rationale Z_A from input such that, when Z_A is fed into the same predictor p, it yields a prediction label flipped from its original label. Continuing the previous example in Figure 2, the generator g selects the "." from a positive input X^1 with label 1 as Z. Consequently, the predictor p learns to treat the presence of "." in Z as an indicative feature for positive classification. On the other hand, the goal of g_a is to select an attack rationale Z_A from a negative input X^0 with a label 0 in such a way that, when Z_A is fed to the same predictor p, the prediction result flips from its original

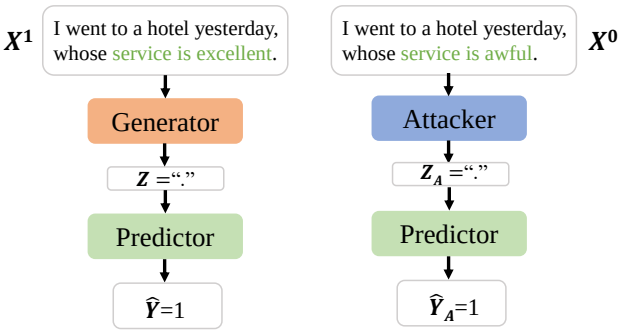

Figure 7. An example of how the attacker works. X^1, X^0 represent positive and negative texts.

label 0 to 1. Achieving this objective is straightforward: g_a simply needs to mimic g by selecting "." as Z_A. This suggests that if g identifies Z from X^1 as a trivial pattern also present in X^0, then g_a can effortlessly select $Z_A = Z$ from X^0, leading to an easy flip of the prediction label of Z_A to 1 in predictor p. On the other hand, if Z is a genuine positive rationale unique to X^1 and the predictor p classifies it correctly, then g_a would be unable to find a positive rationale from the negative input X^0. Therefore, it is difficult for the predictor p to flip Z_A's label from 0 to 1. Thus, we can leverage the attack generator g_a to assist in inspecting and identifying sampling bias. g_a may easily find a Z_A that flips its predicted label in predictor p from its actual label, indicating the presence of semantically unrelated trivial patterns in Z.

To further address this issue, we propose a method to instruct the game on better decorrelation. As illustrated by the previous example, when there is a sampling bias issue, the attack generator g_a surely selects a Z_A that is a trivial pattern lacking semantic significance. For a reasonable predictor p that can accurately classify the real rationale, Z_A is akin to noise, and its classification result should be random and not biased towards any label. Therefore, we introduce a constraint on the predictor p to guide it, ensuring that the classification result for Z_A remains as random as possible. This constraint serves as an ongoing guidance to adjust and correct the behavior of predictor p. An improved predictor p can, in turn, better instruct and guide the updates for the generator g.

A.3. Implementation details of Equation (6) and (7)

For a batch of (X, Y), we first send X to both the generator and the attacker and get Z, Z_A:

$$\begin{aligned} Z &= f_g(X) \\ Z_A &= f_a(X). \end{aligned} \tag{12}$$

Table 5. Statistics of datasets used in this paper

Datasets		Train			Dev			Annotation			
		Pos	Neg	avg_len	Pos	Neg	avg_len	Pos	Neg	avg_len	S
Beer	Appearance	16891	16891	141	6628	2103	145	923	13	126	18.5
	Aroma	15169	15169	144	6579	2218	147	848	29	127	15.6
	Palate	13652	13652	147	6740	2000	149	785	20	128	12.4
Hotel	Location	7236	7236	151	906	906	152	104	96	155	8.5
	Service	50742	50742	154	6344	6344	153	101	99	152	11.5
	Cleanliness	75049	75049	144	9382	9382	144	99	101	147	8.9

Then, we get a copy of Z_A with the pytorch function "torch.detach()":

$$Z'_A = \text{torch.detach}(Z_A). \tag{13}$$

Then we get $\hat{Y}$ and $\hat{Y}'_A$:

$$\begin{aligned} \hat{Y} &= f_p(Z) \\ \hat{Y}'_A &= f_p(Z'_A) \end{aligned} \tag{14}$$

Then we can update the generator and the predictor with

$$\min_{\theta_g,\theta_p} H_c(Y,\hat{Y}) + \min_{\theta_p} H_c([0.5,0.5],\hat{Y}'_A) \tag{15}$$

Note that this updating process will not influence the attacker, since we have used "torch.detach()" for Z_A.

Then, we fix the parameters of the generator and the predictor, and only update the attacker. We get $\hat{Y}_A$ with

$$\hat{Y}_A = f_p(Z_A). \tag{16}$$

Then, we update the attacker with

$$\min_{\theta_a} H_c(1-Y,\hat{Y}_A). \tag{17}$$

Then, we get into the next round to update the generator and the predictor again.

A.4. Datasets

We employ six widely used text classification datasets collected from two rationalization benchmarks. Beer-Appearance, Beer-Aroma, Beer-Palate (which discuss the appearance, aroma, and palate of beer, respectively. They are from the BeerAdvocate (McAuley et al., 2012) benchmark), Hotel-Location, Hotel-Service, Hotel-Cleanliness (which discuss the location, service, and cleanliness of hotels, respectively. They are from the HotelReviews (Wang et al., 2010) benchmark). Among them, the beer-related datasets are most important and used by nearly all of previous research in the field of rationalization. These datasets have human-annotated ground-truth rationales on the test sets for evaluation. But the training sets have only the classification labels and models are trained to extract rationales in an unsupervised way.

For the three beer-related datasets, users need to consult the original authors (McAuley et al., 2012) for permission first.

The statistics of the datasets are in Table 5. Pos and Neg denote the number of positive and negative examples in each set. S denotes the average percentage of tokens in human-annotated rationales to the whole texts. avg_len denotes the average length of a text sequence.

Note that there are two versions of the BeerAdvocate benchmark. The raw datasets in the original BeerAdvocate contain many spurious correlations. However, as we are investigating the model-added spurious correlations in clean datasets, we follow FR to use the version where the inherent spurious correlations in the datasets have been manually cleaned by (Lei et al., 2016).

For the graph classification dataset BA2Motif, we do node level selection on it. That is to say, we select several nodes from a graph to form a subgraph to serve as the rationale.

A.5. Implementation details

We keep the major settings consistent with Inter_RAT and FR, which are commonly utilized in the field of rationalization (Chang et al., 2020; Yu et al., 2021; Liu et al., 2022; Yue et al., 2023). Specifically, we employ the 100-dimensional GloVe (Pennington et al., 2014) for word embedding and 200-dimensional GRUs (Cho et al., 2014) to obtain text representation. The re-parameterization trick for binarized selection is Gumbel-softmax (Jang et al., 2017). Then, we also follow CR to conduct experiments that replace GRUs with pretrained BERT (Devlin et al., 2019) ("bert-based-uncased") and compare with some recent methods that have already been implemented with BERT as a supplement. The random seed is kept the same (the seed is 12252018, inherited from the code of FR) across all the experiments on text classification, as we think experiments with multiple datasets and multiple sparsity settings (totally 12 settings in

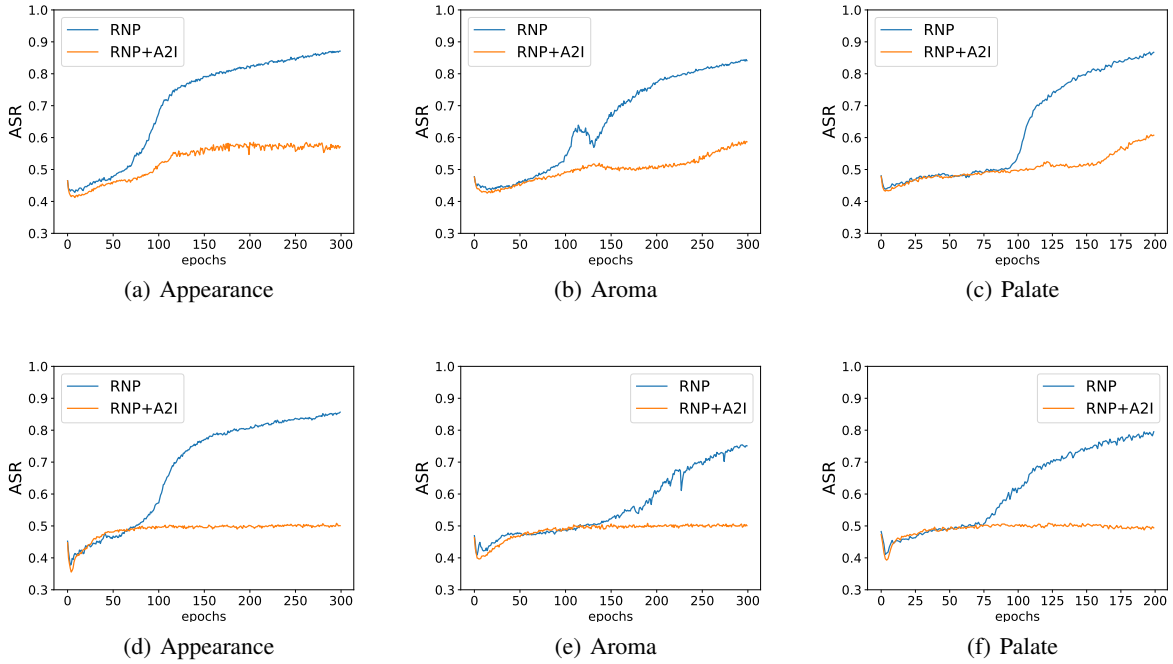

(a) Appearance (b) Aroma (c) Palate

(d) Appearance (e) Aroma (f) Palate

Figure 8. Attack success rate (ASR) on the three beer-related datasets. The rationale sparsity is about 10% (a,b,c) and 30% (d,e,f).

Table 1 and 2) under the same random seed are sufficient to verify the significance of improvement. For the BA2Motifs, we use a two-layer GCN to replace GRUs. The training of GCN is not as stable as GRUs, we report the average results of five random seeds.

Because Inter_RAT, NIR, and CR are methods specifically designed for text tasks and are not suitable for graph tasks, we only compare our A2I with RNP and FR on the BA2Motifs dataset.

The maximum sequence length is set to 256. We use the Adam optimizer (Kingma & Ba, 2015) with its default parameters, except for the learning rate (the learning rate is 0.0001). The temperature for gumbel-softmax is the default value 1. We implement the code with Pytorch on a RTX3090 GPU.

Hyperparameters. For all datasets, we use a learning rate of 0.0001. It is found by manually tune the standard RNP and are applied to both NIR, FR, our A2I, as they are all variants of RNP. The core idea of NIR is to inject noise into the selected rationales. We use RNP as its backbone. A unique hyperparameter of NIR is the proportion of noise. Following the method in the original paper, we searched within $[0.1, 0.2, 0.3]$ and found that 0.1 yielded the best results on most datasets, hence we adopted 0.1 for it. We found that the training of Inter_RAT is very unstable. To avoid potential unfair factors, our main settings are determined with reference to it. Except for the part about sparsity, we used its original hyperparameters for it.

For CR, we just keep the major settings ("bert-base-uncased", the Beer-Appearance dataset, and the sprasity of 10%, removing the coherence regularizer) the same as it and copy its results from its original paper.

Compactness and coherence. For the compactness and coherence regularizers introduced in Equation (4), we adopt both compactness and coherence regularizers to the generator to make the selected rationales human-intelligible. We apply a compactness regularizer term to the attacker to make the attack rationale more similar to the original rationale, thus making it easier to deceive the predictor. However, we do not employ a coherence regularizer on it because we think trivial patterns are often discontinuous.

B. More results

B.1. More results about the attack success rate

More results of the attack success rate are shown in Figure 8.

B.2. More results corresponding to Figure 3

Figure 3 has shown the results of one aspect of the *BeerAdvocate* dataset. We show the results of the other two aspects in Figure 9 and 10. The green lines can somewhat reflect how much the true sentiment is contained in the randomly selected rationales. And we see that only the true sentiment

can generalize to the validation set.

C. Technical proofs

C.1. Derivation of Equation (9)

To begin with, we need to introduce two fundamental properties from probability theory.

The first property is a general property for conditional probability. If $0 < P(Y = 1) < 1$, then for $\forall p$, if $0 < p < 1$, we can always find a variable c, such that $P(Y = 1|c) = p$.

Considering our rationalization situation, we can get the following corollary:

Corollary C.1. *If we can construct G in an arbitrary way, and $0 < P(Y = 1|Z = t) < 1$, then we have*

$$\forall 0 < p < 1,\ \exists g_a \in G,\ P(Y = 1|Z = t, g_a) = p. \tag{18}$$

The second property is also a general property for conditional probability. If $P(Y = 1) = 0$, then for any variable c, we always have $P(Y = 1|c) = 0$. This is also a fundamental property in probability theory.

Considering the rationalization situation, let $Z = r_+$, we have

Corollary C.2. *If we can construct G in an arbitrary way, and $P(Y = 0|Z = r_+) = 0$, then we have that there is no $g_a \in G$ that can make $P(Y = 1|Z = r_+, g_a) > 0$.*

C.2. The convergence of Equation (7)

Quantitative analysis We consider the scenario where the model is functioning correctly, meaning the predictor classifies according to the true rationale R. The generator extracts r_+ from X^1, while the attacker extracts r_+ from X^0 (X^0, X^1 denote texts with negative and positive labels, respectively). In the dataset $\mathcal{D}$, we consider the numbers of positive and negative texts are both n.

We only consider $Z = r_+$, and $Z = r_-$ is nothing different.

We rewrite (7) as (L is the loss function and $f_p(r_+)$ is the confidence level of predicting r_+ as positive)

$$\begin{aligned} L = &-\sum_{Y=1,X} \mathbb{1}_{f_g(X=r_+)} \log f_p(r_+) \\ &-\sum_{Y=0,X} \mathbb{1}_{f_a(X=r_+)} 0.5(\log f_p(r_+) \\ &+ \log(1 - f_p(r_+))) \end{aligned} \tag{19}$$

$$\begin{aligned} \frac{\partial L}{\partial f_p(r_+)} = &\frac{-n * \Pr(r_+|Y = 1) - 0.5n * \Pr(r_+|Y = 0)}{f_p(r_+)} \\ &+ \frac{0.5n * \Pr(r_+|Y = 0)}{1 - f_p(r+)} \end{aligned} \tag{20}$$

We consider a scenario starting with $f_p(r_+) = 0.5$, meaning the predictor is unable to classify using the correct rationale, and we examine in which direction the predictor will converge under these circumstances.

Clearly, when $f_p(r_+) = 0.5$, $\frac{\partial L}{\partial f_p(r_+)} < 0$, meaning that the predictor will learn to increase $f_p(r_+)$ to get lower L. So the predictor will learn to predict r_+ as positive.

So, when will it converge? We denote $\Pr(r_+|Y = 1) = P_1$ and $\Pr(r_+|Y = 0) = P_2$. From (20), we have

$$\frac{\partial L}{\partial f_p(r_+)} < 0,\ s.t.,\ f_p(r_+) < 1 - \frac{P_2}{2P_1 + 2P_2}. \tag{21}$$

From Assumption 4.1, we have $P_1 \geq P_2$. So, we know that we will have $f_p(r_+) \geq 0.75$ when the predictor converges (i.e., $\frac{\partial L}{\partial f_p(r_+)} = 0$).

That means even in the worst case, the predictor can still predict r_+ as positive.

Qualitative analysis Actual training would be easier because, in the above discussion, we do not differentiate between positive sentiment appearing in positive class texts and positive sentiment appearing in negative class texts. In reality, although both are denoted as r_+, they are somewhat distinct.

Here are some practical scenarios where a text contains both positive and negative sentiments.

First, the X labelled with $Y = 1$ may be a combination of strong positive sentiment and weak negative sentiment. A dataset may consists of two kind of sentiment: strong and weak, each of which can be divided to positive and negative. The label of X is decided by the strong sentiment. In this scenario, the attacker may find the weak negative sentiment from X labelled with $Y = 1$, and ask the predictor to classify the weak negative sentiment as neutral. If weak sentiment and strong sentiment have different styles, the attacker here still helps the predictor to focus on strong sentiment and ignore the weak sentiment. As a result, the generator will only select the strong sentiment.

Second, the sentiment may be multi-aspect. For example, a person may have positive sentiment about the beer's appearance, while negative sentiment about the taste. If we are discussing the beer's appearance, the text will still be annotated as positive. In such a scenario, the attacker will try to find the negative comment about the taste, and force the predictor to classify it as neutral. However, this is just what we want. It helps the predictor focus not only on the vanilla sentiment, but also on the aspect (which is included in the context of the sentiment) in which we are interested. Since the predictor classifies the comment about the taste as neutral, it will give the only the feedback about the beer's appearance, which can help the generator focus more on the

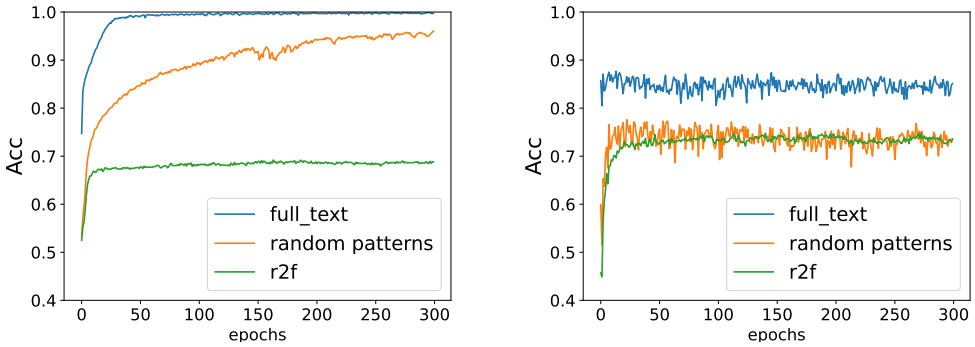

(a) Training (b) Validation

Figure 9. Experiments on the *Appearance* of the BeerAdvocate dataset. The settings are the same as those in Figure 3.

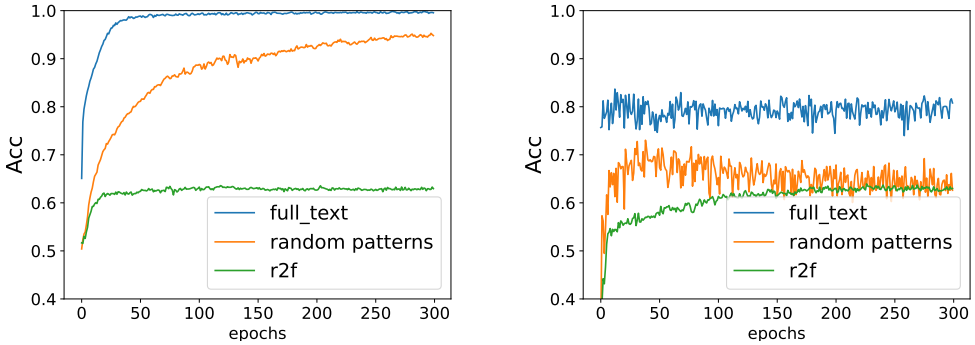

(a) Training (b) Validation

Figure 10. Experiments on the *Palate* of the BeerAdvocate dataset. The settings are the same as those in Figure 3.

appearance.

The above intuitive analysis is somewhat supported by the empirical results in Figure 6. For RNP+A2I, the attack success rate is about 50%, meaning random classification of Z_A. This suggests that the predictor does not predict the Z_A extracted by the attacker to the target class.

C.3. The minimum cross-entropy is equal to entropy

$$H_c(Y,\hat{Y}|Z) = H(Y|Z) + D_{KL}(P(Y|Z)\|P(\hat{Y}|Z)). \quad (22)$$

We have $D_{KL}(P(Y|Z)\|P(\hat{Y}|Z)) \geq 0$ with the equality holds if and only if $P(Y|Z) = P(\hat{Y}|Z)$. As a result, we have

$$\min H_c(Y,\hat{Y}|Z) = H(Y|Z). \quad (23)$$

D. The rationales extracted by llama-3.1-8b-instruct

To further show the potential impact of rationalization in the era of LLMs, here we present the results of the experiments conducted with the llama-3.1-8b-instruct model. We perform both 2-shot prompting and supervised fine-tuning.

For 2-shot prompting, we provide the model with a negative text with its corresponding rationale, and a positive text with its corresponding rationale. For supervised fine-tuning, the supervison label is the classification label, since we perform unsupervised rationale extraction. We use 4*RTX 4090 24GB GPUs and LoRA to fine tune the models.

In most cases, the model can output the rationale in the correct format. Figure 11 shows an example. But in 2-shot prompting, the model sometimes outputs additional parts along with the rationale (through manual observation, this situation does not occur frequently.). Figure 12 is another example. In such cases, we use gpt-3.5-turbo to extract the content within the quotation marks.

Table 6. The comparison between our A2I-based methods (implemented with GRUs, which corresponds to the results in Table 1) and a representative LLM llama-3.1-8b-instruct. The **bold** results means the situations where A2I-based methods outperforms llama (in terms of F1 score).

(a) Results on datasets from the BeerAdvocate benchmark.

Datasets / Methods	Beer-Appearance				Beer-Aroma				Beer-Palate			
	S	P	R	F1	S	P	R	F1	S	P	R	F1
llama (finetune)	n/a	86.3	46.2	60.2	n/a	73.2	50.6	59.8	n/a	61.7	42.6	50.4
llama (2 shot)	n/a	15.4	16.0	15.7	n/a	17.9	24.2	20.6	n/a	13.0	22.2	16.4
RNP+A2I	10.8	78.3	45.8	57.8	9.8	86.0	54.3	**66.6**	10.9	66.3	58.2	**62.0**
FR+A2I	11.3	76.0	46.5	57.7	10.0	85.7	54.8	**66.9**	9.7	71.4	55.8	**62.6**
RNP+A2I	20.0	73.3	79.4	**76.2**	19.5	49.0	61.4	54.5	19.4	49.0	76.4	**59.7**
FR+A2I	19.8	80.0	85.6	**82.7**	19.4	64.2	80.0	**71.2**	19.2	44.2	68.2	**53.7**
RNP+A2I	29.9	59.3	95.9	**73.3**	27.8	44.5	79.3	57.0	30.5	30.8	75.5	43.7
FR+A2I	28.8	61.3	95.3	**74.6**	30.9	41.4	82.2	55.1	29.1	31.6	73.8	44.2

(b) Results on datasets from the HotelReview benchmark.

Datasets / Methods	Hotel-Location				Hotel-Service				Hotel-Cleanliness			
	S	P	R	F1	S	P	R	F1	S	P	R	F1
llama-3.1-8b (finetune)	n/a	58.6	39.0	46.8	n/a	77.3	40.6	53.3	n/a	54.9	31.3	39.9
llama-3.1-8b (2 shot)	n/a	45.8	59.1	51.6	n/a	45.3	51.7	48.3	n/a	39.3	43.0	41.1
RNP+A2I	9.0	50.2	53.4	**51.7**	11.6	46.8	47.4	47.1	9.7	34.7	38.2	36.4
FR+A2I	9.9	53.2	62.1	**57.3**	11.5	47.7	47.7	47.7	10.8	35.9	43.7	39.4

Task: Sentiment classification about Beer's appearance
Input: Pours a rather crisp yellow almost orange with a thin head. The aroma is dominated by sweet malts with just a slight hoppiness dancing in the background. The taste does have a surprising amount of hoppiness for a Pilsner. There is a good maltiness to it as well, but citrus hops just slightly overpower. The beer is very light and refreshing. This makes for an excellent summer session beer.
Expected output: 1|pours a rather crisp yellow almost orange with a thin head .
llama-3.1 output: 1|pours a rather crisp yellow almost orange

Figure 11. An example of llama's output. Here "1" means that the class label Y is positive. And the words after "|" represent the rationale.

We found that there is a significant likelihood that responses from Llama would not contain explicit "positive/negative" classifications (for instance, in the hotel-location dataset, 50.5% of responses from the llama-finetune model did not specify a category, and this figure was 53.0% for hotel-cleanliness dataset). If we were to consider these responses without clear categories as incorrect predictions, the accuracy would appear very low and could be misleading. Considering that our main comparison is on the rationale quality and we do not claim our classification ability is superior to LLMs, hence we do not report this prediction accuracy to avoid unnecessary confusion.

The results are shown in Table 6. LLMs are not good at counting, so we did not constrain the percentage length (i.e., sparsity) of the rationale extracted by the model. We do not report the prediction accuracy for llama because we find that there is a significant likelihood that responses from Llama would not contain explicit "positive/negative" classifications (for instance, in the hotel-service dataset, 50.5% of responses from the llama-finetune model did not specify a category, and this figure was 53.0% for hotel-cleanliness dataset). If we were to consider these responses without clear categories as incorrect predictions, the accuracy would appear very low and could be misleading. Considering that

Task: Sentiment classification about Beer's appearance
Input: 22oz bottle pouted into a Goblet: Opaque orange with a light, white, creamy head that was not all that well retained but full of carbonation, but did settle into a small thin cap. The aroma was more Belgian triple than IPA, Sweet and malty. The taste is a very nice balance of the two styles. A little more hops, but balanced very nice with the sweetness of the malt and fruit. The beer had a medium to full body, perhaps a little too thick for my taste, but still good. The beer had a nice bitter dry aftertaste and was well carbonated. The beer was fairly easy to drink give the ABV, but after the 22oz, I was pretty well done. Overall, a good beer and probably the first one of the side projects that I think the brewery should consider brewing on a regular basis.
Expected output: 1|opaque orange with a light , white , creamy head that was not all that well retained but full of carbonation , but did settle into a small thin cap .
llama-3.1 output: positive|The overall tone of the review is positive, with phrases such as "a very nice balance of the two styles", "nice bitter dry aftertaste", "well carbonated", and "overall, a good beer" indicating a favorable opinion of the beer.
GPT-3.5-restructured output: 1|a very nice balance of the two styles nice bitter dry aftertaste well carbonated overall, a good beer

Figure 12. An example of llama fails to output the rationale in the right format.

our main comparison is on the rationale quality and we do not claim our classification ability is superior to LLMs, hence we do not report this prediction accuracy to avoid unnecessary confusion.

Comparing the results of the supervised fine-tuned llama-3.1 with our results in Table 1, llama-3.1 does not have a crushing advantage. For example, on the Beer-Aroma dataset, FR+A2I outperforms llama-3.1 at sparsity levels of 10% and 20%. Similarly, on the Beer-Palate dataset, RNP+A2I also outperforms llama-3.1 at sparsity levels of 10% and 20%. Besides, our A2I can be applied to graph data, while it is not easy to do so for LLMs.

E. Connection to More Fields

As deep learning progresses, enhancing few-shot learning (Tong et al., 2024b;a; 2025b) and improving the efficiency of multi-modal large language models (MLLMs) (Tong et al., 2025a; Wang et al., 2025; Cui et al., 2025) are becoming key challenges. With the rapid development of deep learning techniques, neural network-based methods (Zheng et al., 2023; Sun et al., 2024b; Zheng et al., 2024a;b) and LLM-based methods (Zheng et al., 2025; Zheng & Lee, 2025) demonstrate superior performances on a wide range of applications and optimization tasks. We acknowledge their growing importance and consider it a promising direction for future extensions of our method.